

ISOTHERMAL ADSORPTION CHARACTERISTICS OF BIORETENTION MEDIA FOR FECAL *Escherichia Coli*

by

**Ying MEI^{a*}, Hang ZHOU^a, Xiao-Han ZHU^a, Peng ZHANG^b,
Xiao-Fei LI^c, Yi-Ming ZUO^d, Xiu-Mei WANG^a, and Jun-Jiang BAO^a**

^a Department of Environmental Science and Engineering,
School of Energy and Power Engineering, Inner Mongolia University of Technology, Hohhot, China

^b PetroChina Shanxi Yangquan Marketing Company, Yangquan, China

^c College of Chemical Technology, Beijing University of Chemical Technology, Beijing, China

^d School of Ecology and Environment, Inner Mongolia University, Hohhot, China

Original scientific paper

<https://doi.org/10.2298/TSCI2004427M>

*Rainfall runoff contains a huge number of pathogenic bacteria that seriously deteriorate water quality. Bioretention is an effective approach to removal of pathogenic bacteria from rainwater. This study uses sandy soil, fly ash, slag, sandy soil+5% fly ash, and sandy soil+5% slag as media to evaluate the adsorption of fecal *Escherichia coli*. The mechanisms of the five media conform to the Langmuir's isotherm adsorption equation, and a pseudo-first-order kinetic model is adopted to reveal the adsorption kinetics.*

Key words: bioretention, media, *Escherichia coli*, bacteria adsorption

Introduction

With the rapid development of cities, vegetation and low-lying lands, that contain water and exhibit the capability to permeate water, are being rapidly replaced with bituminous streets, parking lots, and buildings that cannot permeate water, thereby increasing permeated areas and deteriorating the quality of rainfall water. Consequently, the problems of flooding events and insufficient water resources have become increasingly serious [1, 2]. Furthermore, non-point source (NPS) pollution has elicited considerable attention [3-5]. Rainfall runoff plays an important role in NPS pollution [5]. Pollutant concentration in rainfall runoff contains total particles, organic matter (OM), heavy metals, pathogenic bacteria, and other harmful materials. All these pollutants lead to serious environmental issues [6]. At present, controlling NPS pollution is the major direction taken to protect the water environment of a city [7]. Best management practices (BMP) are common solutions used to control NPS pollution, and exhibit high particle removal efficiency [8]. Bioretention, sometimes also called as a rain garden, is a BMP technique used to reduce rainfall runoff and flood peak and to improve the water quality of rainfall runoff [9]. Bioretention is frequently adopted and is considered the best rainfall treatment method due to its high efficiency. In general, a bioretention area includes plants, soil, covering, coarse sand, gravel and a drainage system at the bottom [10, 11]. Among these components, soil plays an important role in reducing pollutants in rainfall runoff [12]. Hence, a suitable soil type should be selected as bioretention media to control NPS pol-

* Corresponding author, e-mail: hanmy79@163.com

lution, which is the focus of the current work. In previous studies, most researchers have used a model to evaluate the performance of BMP in removing pollutants [7]. In addition, many researchers have focused on the removal of heavy metals and nutrients, whereas the removal of pathogenic bacteria and the impact factors of NPS pollution control have been rarely investigated [13, 14]. The number of pathogenic bacteria is a key indicator used to evaluate drinking and recreational water. Fecal *Escherichia coli* (FC) is a frequently used indicator of pathogenic bacteria [11]. The FC, which is a subspecies of total coliform, originates from the digestive tract of humans and animals. The FC does not normally cause diseases by itself, and it can indicate the existence of other types of pathogenic bacteria. Accordingly, the kinetic mechanism of pathogenic bacteria in BMP and their impact factors should be investigated.

This study evaluates the adsorption effects of several types of bioretention media. Its results can be served as an important reference when selecting media. After considering the different adsorption capabilities, a suitable media type can be selected to improve the efficiency of pathogenic bacteria removal. Therefore, this study uses different adsorption equations to determine the adsorption capabilities of several typical media (*e. g.*, sandy soil, fly ash, and slag). In addition, this study considers pH and ion strength as impact factors of adsorption. The kinetics of absorption is also analyzed.

Materials and methods

Materials

Five types of media, namely, sandy soil, fly ash, slag, sandy soil+5% fly ash, and sandy soil+5% slag, were used and their adsorption capabilities were evaluated. The physical and chemical characteristics of the five media are presented in tab. 1. After smashing, the five media were filtered through a 2 mm screen. Sandy soil+5% fly ash, which was a combination of sandy soil and fly ash, had a volumetric ratio of 19:1. Sandy soil+5% slag was prepared in the same manner. All the media were dried in an oven for 24 hours at 60 °C.

Table 1. Physical and chemical characteristics of different soil types

Media	Size			pH	Organic matter [gkg ⁻¹]
	Sand [%]	Silt [%]	Clay [%]		
Sandy soil	73.26	19.79	6.95	6.59	4.66
Fly ash	35.67	44.95	19.38	8.90	4.73
Slag	89.33	9.60	1.07	7.13	163.58
Sandy soil+5% fly ash	71.09	22.17	6.74	8.57	8.25
Sandy soil+5% slag	77.22	21.37	1.41	7.64	11.33

Water samples contaminated with feces were prepared as follows: first, 20 g fresh cow feces were added to each five 500 mL conical flask; then, 40, 80, 120, 160, and 200 mL asepsis water were added to each conical flask. The samples were shaken in an incubator for 30 minutes. After boiling for 20 minutes, the supernatant was collected and placed in a 1000 mL conical flask to prepare different concentrations of fecal water [7]. The prepared fecal water samples were stored under sterile conditions at a low temperature. To determine the effects of pH and ion strength, HCl and NaOH at 0.1 mol/L were used to adjust pH, whereas

KCl was used to adjust ion strength. *Escherichia coli* concentration can be calculated using the following equation:

$$N = \frac{m}{V} \quad (1)$$

where N denotes the concentration of *Escherichia coli*, which is expressed in colony-forming unit (CFU)/mL; m refers to the amount of *Escherichia coli*, and V indicates the sample volume, which is expressed in mL.

Adsorption studies

Six 50 mL conical flasks without bacteria were marked with numbers. Then, 200 mg media were added separately to five conical flasks. Subsequently, 10 mL fecal water with a certain concentration was added to the five conical flasks. After conditioning, the five conical flasks were placed in an incubator at 50 °C and shaken at 180 rpm. Adsorption was completed after 90 minutes. Thereafter, 8 mL water was centrifuged at 2000 rpm for 15 min [15]. A prepared M-FC medium was used to count FC. This process was performed at 44.5±0.5 °C for 24±2 hours. The amount of FC was indicated by color. Equation 1 calculates FC concentration before and after adsorption.

Results and discussions

Isothermal sorption of fecal coliforms

An isothermal curve should be drawn to describe the adsorption process and determine the maximum adsorption and adsorption kinetics of the five types of media. The current study used the Langmuir [15, 16], Freundlich [17, 18], and Flory-Huggins (F-H) models [19].

Langmuir isotherm

The Langmuir equation is expressed as [20]:

$$\frac{1}{q_e} = \frac{1}{bq_{\max}C_e} + \frac{1}{q_{\max}} \quad (2)$$

where q_e refers to the adsorption amount in unit volume at adsorption equilibrium (CFU mL⁻¹), q_{\max} – the saturated adsorption amount of a single layer (CFU mL⁻¹), b – a constant parameter (CFU/mL), and c_e – the FC concentration at adsorption equilibrium (CFU mL⁻¹). The R_L is a key parameter without unit, which can be calculated:

$$R_L = \frac{1}{1 + (1 + bC_0)} \quad (3)$$

where C_0 denotes the initial FC concentration in a solution (CFU mL⁻¹), and b is a constant parameter (mL CFU⁻¹).

In the Langmuir isotherm model, the amounts of single-layer adsorption q_{\max} and constant b are listed in tab. 2. The coefficient of determination, R^2 , is higher than 0.9. From the calculation results of the Langmuir equation, the adsorption amounts of the five media decrease in the following order: sandy soil+5% fly ash (2439 CFU mL⁻¹) > sandy soil+5% slag (1923 CFU mL⁻¹) > fly ash (952 CFU mL⁻¹) > sandy soil (355 CFU mL⁻¹) > slag (168 CFU mL⁻¹).

The R_L is dimensionless adsorption strength. The FC absorption is irreversible when $R_L = 0$ and reversible when $0 < R_L < 1$. The process cannot be performed when $R_L > 1$. From the R_L results calculated using eq. (2), all the adsorption processes of the five media are reversible, and thus, these media can be considered good FC adsorbents.

Table 2. The FC adsorption amount and Langmuir isothermal parameters

Media	q_{\max} [CFU mL ⁻¹]	B [10 ⁻³ mL CFU ⁻¹]	R_L	Equation	R^2
Sandy soil	952	6.25	$0 < R_L < 1$	$y = -0.168x + 0.00105$	0.9773
Fly ash	168	26.53	$0 < R_L < 1$	$y = -0.2244x + 0.0060$	0.9256
Slag	355	7.26	$0 < R_L < 1$	$y = -0.3882x + 0.0028$	0.9812
Sandy soil+5% fly ash	2439	0.085	$0 < R_L < 1$	$y = 4.8485x + 0.00041$	0.9374
Sandy soil+5% slag	1923	0.026	$0 < R_L < 1$	$y = 20.1136x + 0.00052$	0.9923

Freundlich isotherm

The Freundlich isotherm equation is expressed as [21]:

$$q_e = K_f C_e^{1/n} \quad (4)$$

After converting eq. (4) via a logarithm, the equation is transformed into:

$$\ln q_e = \ln K_f + \frac{1}{n} \ln C_e \quad (5)$$

where K_f and n are constants, and the remaining parameters are the same as those in eq. (4).

From the FC adsorption results of the five media, the simulation results of the Freundlich isotherm equation are presented in tab. 2. The K_f values of the five media are as follows: slag (2279.2 CFU mL⁻¹), sandy soil+5% slag (203.20 CFU mL⁻¹), fly ash (8.6803 CFU mL⁻¹), sandy soil (0.0204 CFU mL⁻¹), and sandy soil+5% fly ash (0.0011 CFU mL⁻¹). A high K_f indicates strong adsorption capability. The order of adsorption capability from highest to lowest is as follows: sandy soil+5% fly ash, sandy soil+5% slag, fly ash, sandy soil, and slag. This result complies with the Langmuir isotherm equation.

The results of Ramesh *et al.* [22] showed that n between 1 and 10 indicates a positive adsorption process. As provided in tab. 3, the n values of fly ash, sandy soil+5% fly ash, and sandy soil+5% slag are 1.0694, 9.2851, and 9.5238, respectively. Thus, the three media are good in absorbing FC in water.

Table 3. Parameters of the Freundlich isotherm for FC adsorption

Media	K_f [CFU mL ⁻¹]	n	Equation	R^2
Sandy soil	8.6803	1.0694	$y = -0.0473x + 0.484$	0.8495
Fly ash	2279.2	9.2851	$y = -0.194x + 0.295$	0.9184
Slag	0.0204	0.8275	$y = -0.386x + 8.284$	0.8275
Sandy soil+5% fly ash	0.0011	0.5952	$y = -0.355x + 11.497$	0.9936

Sandy soil+5% slag	203.20	9.5238	$y = -2.453x + 21.283$	0.9274
--------------------	--------	--------	------------------------	--------

As shown in tabs. 2 and 3, sandy soil+5% fly ash has the highest FC adsorption capacity and it exhibits favorable FC adsorption characteristics. Thus, it is the preferred FC adsorbent. In addition, the Langmuir adsorption isotherm model is better than the Freundlich adsorption model in fitting the FC adsorption of the five types of media based on the model correlation coefficients given in tabs. 2 and 3. With the exception of the honeycomb slag, the FC adsorption of the four other media is in accordance with the Langmuir adsorption isotherm, which indicates that the FC adsorption of the four media is single-layer adsorption.

The F-H model

The F-H model is expressed as follows:

$$\log \frac{Q}{C_0} = \log K_{FH} + n_{FH} \log(1 - Q) \quad (6)$$

where K_{FH} is a constant parameter, n_{FH} – the amount of adsorbents used during adsorption, and Q – the surface covering rate:

$$Q = 1 - \frac{C_e}{C_0} \quad (7)$$

When eqs. (7) and (6) are combined:

$$\log \frac{C_0 - C_e}{C^2} = \log K_{FH} + n_{FH} + n_{FH} \log \frac{C_e}{C_0} \quad (8)$$

where C_0 and C_e denote the initial concentration and the concentration after adsorption equilibrium [mgL^{-1}], respectively.

In addition, the equilibrium constant, K_{FH} , is used to calculate the Gibbs free energy:

$$\Delta G = -2.303RT \log K_{FH} \quad (9)$$

where T [K] is the absolute temperature, and $R = 8.314 \text{ J/molK}$. Gibbs free energy ΔG is used to evaluate the characteristic of FC adsorption by soil.

The results of FC adsorption simulated by F-H at $25 \text{ }^\circ\text{C}$ and $\text{pH} = 7.0$ are provided in tab. 4. sandy soil has a relative K_{FH} , and its adsorption speed is faster than those of the four other types of media. A positive ΔG indicates that FC adsorption is deliberate. For the comparison of the n_{FH} of the media, the FC adsorption capabilities of the five media types decrease in the following order: sandy soil, sandy soil+5% fly ash, sandy soil+5% slag, fly ash, and slag.

The comparison of the five media in terms of the FC adsorption parameter n_{FH} shows that sand exhibits the strongest FC binding capacity, which is inconsistent with the results of the first two adsorption isotherm models. This inconsistency is attributed to the assumption that different models vary and are caused by various adsorption systems. The adsorption characteristics of different adsorbent materials on FC are related to the structure, functional groups, and surface area of the adsorbed material. The adsorption mechanism of various adsorbent materials on FC will be investigated in future studies.

Table 4. Parameters of the F-H model during adsorption simulation at 25 °C and pH = 7.0

Media	n_{FH}	K_{FH}	ΔG [kJmol ⁻¹]	R^2
Sandy soil	-1.2714	0.0000177	27.109	0.9428
Fly ash	-4.5326	0.0000024	32.044	0.7857
Slag	33.1923	0.00082	17.621	0.9535
Sandy soil+5% fly ash	3.7207	0.000126	22.259	0.8759
Sandy soil+5% slag	1.3144	0.0000132	27.841	0.9214

Adsorption results under different impact factors

The pH

This study evaluates the FC adsorption results of the five media within the pH range of 3-10. The adsorption amount of the five media is expressed using a Gaussian equation, as shown in fig. 1. The optimal adsorption amount of the five media is obtained at pH = 3. The FC adsorption amount initially decreases and then increases with increasing pH. Sandy soil, fly ash, sandy soil+5% fly ash, and sandy soil+5% slag have the lowest adsorption amount when pH = 6. As the distribution coefficient of FC in the media, K_d is a key parameter of adsorption capability. Figure 2 shows K_d at different pH values, which is calculated:

$$K_d = \frac{q_e}{C_0} \quad (10)$$

where q_e refers to the adsorption amount in fixed volume at adsorption equilibrium (CFU/mL) and C_0 is the initial FC concentration (CFU/mL). As shown in fig. 2, K_d is negatively proportional to pH when pH is between 3 and 6, except for slag. By contrast, K_d is positively proportional to pH at a pH range of 6.0-10.0, thereby indicating that adsorption amount decreases with increasing pH. At various pH values, sandy soil, sandy soil+5% fly ash, and sandy soil+5% slag exhibit strong adsorption capabilities, whereas fly ash and slag have weak adsorption capabilities. Sandy soil+5% slag has the lowest K_d of 56.5% and an average value of 83.1%. Compared with those of sandy soil+5% slag, the maximum K_d of slag is 82% and its average is 31.3%.

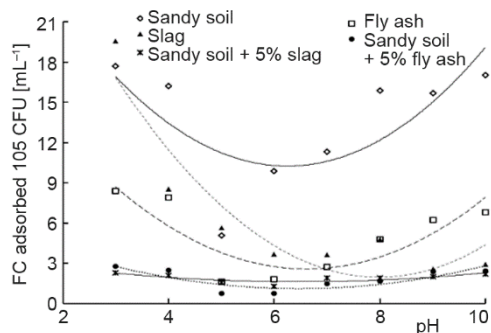


Figure 1. Adsorption performance under various pH values

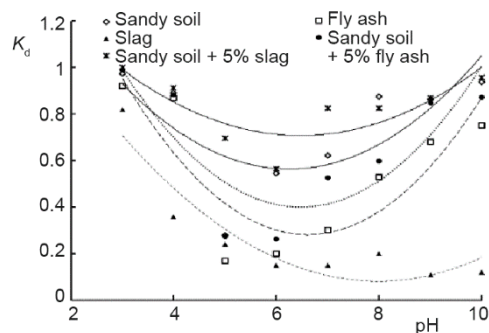


Figure 2. Variation of distribution of parameter K_d with pH

Ion strength

The FC adsorption amounts of the five media at various ion strengths (KCl, 1-100 mmol/L) are presented in fig. 3. The adsorption amounts of fly ash, slag, and sandy soil+5% fly ash are positively proportional to ion strength. Adsorption amount decreases with increasing ion strength. The absorption amount of sandy soil is positively proportional to ion strength when ion strength ranges from 1-20 mmol/L. However, the relationship is initially negative and then remains constant. For sandy soil+5% fly ash, the relationship between FC adsorption amount and ion strength is positive. In general, an increase in ion strength enhances FC adsorption amount and negatively impacts FC adsorption when ion strength is at a low level (1-20 mmol/L), except for sandy soil+5% fly ash.

Figure 4 shows K_d at different ion strengths calculated using eq. (10). The figure also indicates adsorption capability at different ion strengths. Fly ash and slag have strong FC adsorption capability at low ion strength. By contrast, sandy soil+5% fly ash and sandy soil+5% slag have strong FC adsorption capability at high ion strength. However, sandy soil does not exhibit good absorption performance within the entire range.

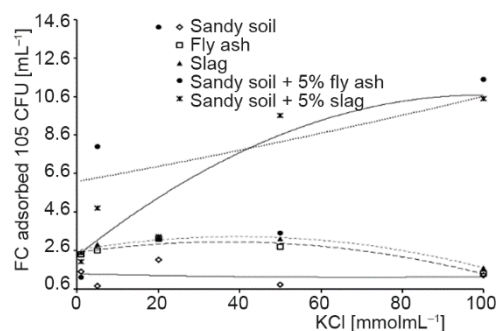


Figure 3. Adsorption amount at different ion strengths

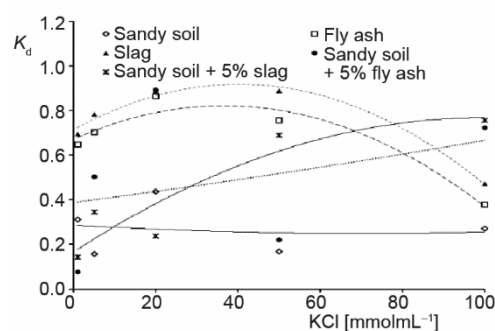


Figure 4. Variation of distribution of parameter K_d with ion strength

Discussion

Numerous impact factors, such as the surface characteristics of adsorbents, surface characteristics of bacteria, liquid characteristics, and the external environment are observed during bacterial adsorption. In general, the interaction between bacteria and a solid surface can be described on the basis of DLVO theory and zeta potential [23]. The current study evaluates the impact of pH on adsorption performance. The results show that FC adsorption amount decreases with increasing pH within the range of 3-6. This finding is similar to the results of Wu *et al.* [24] and Jiang *et al.* [25]. Large amounts of H^+ enter the shear layer between bacteria and solid when pH is within a low range and the amount of H^+ increases, thereby increasing zeta potential (from a negative value to zero). Consequently, the electrostatic repulsion between FC and solids decreases, which aids the adsorption of FC onto the surface of solids. This condition complies with DLVO theory [26].

Meanwhile, the adsorption amount of the media (except for slag) increases with increasing pH from 6 to 10, which does not agree with DLVO theory. The electrostatic attraction between FC and solids is not a dominant factor, or the surface charge of solids is changed.

Ion strength in the liquid can impact the double-layer thickness of FC and solids, which determines the distance between FC and solids. Figure 3 shows that the results can be

easily explained by DLVO theory. Adsorption amount and capability become negative with increasing ion strength from 50-100 mmol mL⁻¹. This condition can be attributed to a minimum double-layer thickness, in which electrostatic forces are not major factors in FC adsorption.

Kinetic experiment results of FC adsorption in different types of media

First-order kinetic model

The first-order kinetic model is:

$$\frac{dq_t}{dt} = k_1(q_e - q_t) \quad (11)$$

where q_t is the adsorption amount with a fix adsorbent amount at time t (CFU mL⁻¹), and k_1 [min⁻¹] – the speed constant of the first-order kinetic model.

Second-order kinetic model

The second order kinetic model is:

$$\frac{dq_t}{dt} = k_2(q_e - q_t)^2 \quad (12)$$

where q_t and q_e are the same as those in eq. (11), and k_2 [CFU mL⁻¹h⁻¹] is the speed constant of the second-order kinetic model.

The first-order and second-order models can express the kinetic characteristics of the pollutant adsorption isotherm, which estimates the adsorption amount and the required time of adsorption equilibrium. The parameters k_2 , R^2 , and $q_{e(\text{model})}$ of the first-order and second-order kinetic models and the calculation results are provided in tab. 5. This table indicates that the first-order model is more suitable for the kinetics of FC adsorption than the second-order kinetic model. Therefore, the FC adsorption of the five media complies with the first-order kinetic model.

Table 5. Calculation results of the first-order and second-order kinetic models at 298 K

Media	First-order kinetic model		Second-order kinetic model			
	R^2	q_e [10 ⁴ CFU mL ⁻¹]	k_1 [CFU mL ⁻¹ h ⁻¹]	R^2	q_e [10 ⁶ CFU mL ⁻¹]	k_2 [10 ⁻⁶ CFU mL ⁻¹ h ⁻¹]
Sandy soil	0.919	9.705	0.3756	0.829	1.337	-0.540
Fly ash	0.944	6.460	0.1783	0.900	1.484	-0.671
Slag	0.975	10.066	0.4267	0.861	2.732	-0.352
Sandy soil+5% fly ash	0.986	5.418	0.2148	0.922	2.469	-0.463
Sandy soil+5% slag	0.966	45.63	0.1313	0.982	1.314	-0.791

Conclusion

In this paper we ignore the effect of porous size on the kinetic property, Liu's fractal modification [27, 28] is a suitable tool to studying the porosity effect by the fractal calculus [29-33].

The adsorption of fecal coliform by five types of media highly complies with the Langmuir adsorption isotherm. On the basis of the Langmuir equation, the adsorption amounts of the five types of media decrease in the following order: sandy soil+5% fly ash (2439 CFU mL⁻¹), sandy soil+5% slag (1923 CFU mL⁻¹), fly ash (952 CFU mL⁻¹), sandy soil (355 CFU mL⁻¹), and slag (168 CFU mL⁻¹). The fecal coliform adsorption of the five types of media is positive at an R_L range of 0-1, which indicates that single-layer adsorption is dominant. On the basis of K_F and n_{KF} calculated via the Freundlich isotherm, the fecal coliform adsorption capabilities of the five types of media decrease in the following order: sandy soil+5% fly ash, sandy soil+5% slag, fly ash, sandy soil, and slag. The n values of fly ash, sandy soil+5% fly ash, and sandy soil+5% slag are 1.0694, 9.2851, and 9.5238, respectively. Therefore, the three types of media exhibit good fecal coliform adsorption in liquid. The average free energy of fecal coliform adsorption by the five types of media is lower than 8 kJ/mol, thereby indicating that physical adsorption is dominant and deliberate. Within the pH range of 3-10, the optimal adsorption amount of fecal coliform occurs at pH = 3.0. The adsorption amount of fecal coliform initially increases and then decreases with increasing pH. The adsorption amount of fecal coliform decreases to the lowest point at pH = 6.0, except in slag. The adsorption amount increases when ion strength range is 1-20 mmol/L. However, adsorption amount decreases with increasing ion strength. The first-order kinetic model is more suitable for simulating the kinetic process of adsorption than the other models based on the simulation results of kinetic adsorption.

Acknowledgment

This work was supported by National Natural Science Foundation of China (No. 21667020) and the Key Project of School Foundation of Inner Mongolia University of Technology (No. 2014219) and Inner Mongolia of China Science and Technology Innovation Guidance Project Plan in 2017: Research and Demonstration on the Implementing Model of Large-scale Dairy Farm Wastewater Returning to Field.

References

- [1] He, J. X., et al., Characterizing Physicochemical Quality of Stormwater Runoff from an Urban Area in Calgary, *Journal of Environmental Engineering*, 136 (2010), 11, pp. 1206-1217
- [2] Karlaviciene, V., et al., The Impact of Storm Water Runoff on a Small Urban Stream, *Journal of Soils and Sediments*, 9 (2009), 1, pp. 6-12
- [3] Brezonik, P. L., et al., Analysis and Predictive Models of Stormwater Runoff Volumes, Loads, and Pollutant Concentrations from Watersheds in the Twin Cities Metropolitan Area, *Water Research*, 36 (2002), 7, pp. 1743-1757
- [4] Gwang, L. J., et al., Optimization of Integrated Urban Wet-Weather Control Strategies, *Journal of Water Resource Planning and Management*, 131 (2005), 4, pp. 307-315
- [5] Li, C., et al., Characterization and First Flush Analysis in Road and Roof Runoff in Shenyang, *Water Science and Technology*, 70 (2014a), 3, pp. 397-406
- [6] Li, C. L., et al., Research Progress on Urban Non-Point Source Pollution, *Chinese Journal of Ecology*, 32 (2010), 3, pp. 492-500
- [7] Nicholas, M., et al., Nonpoint Source Pollution, *Water Environment Research*, 87 (2015), 10, pp. 1576-1594
- [8] Maniquiz, M. C., et al., Long-Term Monitoring of Infiltration Trench for Nonpoint Source Pollution Control, *Water Air Soil Pollution*, 212 (2010), 1-4, pp. 13-26
- [9] LeFevre, G. H., et al., Review of Dissolved Pollutants in Urban Storm Water and Their Removal and Fate in Bioretention Cells, *Journal of Environmental Engineering*, 141 (2015), 1, ID 04014050
- [10] Davis, A. P., et al., Laboratory Study of Biological Retention for Urban Stormwater Management, *Water Environmental Research*, 73 (2001), 1, pp. 5-14

- [11] Rusciano, G. M., Obropta, C. C., Bioretention Column Study: Fecal Coliform and Total Suspended Solids Reductions, *American Society of Agricultural and Biological Engineers*, 50 (2007), 4, pp. 1261-1269
- [12] Lucke, T., Nichols, P. W. B., The Pollution Removal and Stormwater Reduction Performance of Streetside Bioretention Basins After Ten Years in Operation, *Science of the Total Environment*, 536 (2015), Dec., pp. 784-792
- [13] Jang, A., et al., The Removal of Heavy Metals in Urban Runoff by Sorption on Mulch, *Environmental Pollution*, 133 (2005), 1, pp. 117-127
- [14] O'Neill, S. W., et al., Water Treatment Residual as a Bioretention Amendment for Phosphorus. Ii: Long-Term Column Studies, *Journal of Environmental Engineering*, 138 (2012), 3, pp. 328-336
- [15] Guber, A. K., et al., Effect of Bovine Manure on Fecal Coliform Attachment to Soil and Soil Particles of Different Sizes, *Applied and Environmental Microbiology*, 73 (2007), 10, pp. 3363-3370
- [16] Zeng, L., et al., Adsorptive Removal of Phosphate from Aqueous Solutions Using Iron Oxide Tailings. *Water Research*, 38 (2004), 5, pp. 1318-132
- [17] Nasehi, S. M., et al., Removal of Dark Colored Compounds from Date Syrup Using Activated Carbon: a Kinetic Study, *Journal of Food Engineering*, 111 (2012), pp. 490-495
- [18] Triantafyllidis, K. S., et al., Iron-Modified Hydrotalcite-Like Materials As Highly Efficient Phosphate Sorbents, *Journal of Colloid and Interface Science*, 342 (2010), 2, pp. 427-436
- [19] Malana, M. A., et al., Adsorption Studies of Arsenic on Nano Aluminium Doped Manganese Coppe Ferrite Polymer (MA, VA, AA) Composite: Kinetics and Mechanism, *Chemical Engineering Journal*, 172 (2011), 2-3, pp. 721-727
- [20] Golder, A. K., et al., Removal of Phosphate from Aqueous Solutions Using Calcined Metal Hydroxides Sludge Waste Generated from Electrocoagulation, *Separation and Purification Technology*, 52 (2006), 1, pp. 102-109
- [21] Freundlich, H. M. F., Over the Adsorption in Solution, *The Journal of Physical Chemistry*, 57 (1906), pp. 385-471
- [22] Ramesh, A., et al., Adsorption of Inorganic and Organic Arsenic from Aqueous Solutions by Polymeric Al/Fe Modified Montmorillonite, *Separation and Purification Technology*, 56 (2007), 1, pp. 90-100
- [23] Marshall, K., et al., Mechanism of the Initial Events in the Sorption of Marine Bacteria to Surfaces, *Journal of General Microbiology*, 68 (1971), 3, pp. 337-348
- [24] Wu, H., et al., Adsorption of Pseudomonas Putida on Soil Particle Size Fractions: Effects of Solution Chemistry and Organic Matter, *Soils Sediments*, 12 (2012), 2, pp. 143-149
- [25] Jiang, D., et al., Adsorption of Pseudomonas Putida on Clay Minerals and Iron Oxide, *Colloids and Surfaces B-Biointerfaces*, 54 (2007), 2, pp. 217-221
- [26] Rong, X., et al., Interaction of Pseudomonas Putida with Kaolinite and Montmorillonite: a Combination Study by Equilibrium Adsorption., ITC, SEM and FTIR, *Colloids and Surfaces B-Biointerfaces*, 64 (2008), 1, pp. 49-55
- [27] Liu, H. Y., et al., A Fractional Nonlinear System for Release Oscillation of Silver Ions from Hollow Fibers, *Journal of Low Frequency Noise, Vibration and Active Control*, 38 (2018), 1, pp. 88-92
- [28] Liu, H. Y., et al., A Fractal Rate Model for Adsorption Kinetics at Solid/Solution Interface, *Thermal Science*, 23 (2019), 4, pp. 2477-2480
- [29] He, J. H., Ji, F. Y., Two-Scale Mathematics and Fractional Calculus for Thermodynamics, *Thermal Science*, 23 (2019), 4, pp. 2131-2133
- [30] He, J. H., Fractal Calculus and Its Geometrical Explanation, *Results in Physics*, 10 (2018), Sept., pp. 272-276
- [31] Li, X. X., et al., A Fractal Modification Of The Surface Coverage Model For An Electrochemical Arsenic Sensor, *Electrochimica Acta*, 296 (2019), Feb., pp. 491-493
- [32] He, J. H., Ain, Q. T., New Promises and Future Challenges of Fractal Calculus: from Two-Scale Thermodynamics to Fractal Variational Principle, *Thermal Science*, 24 (2020), 2A, pp. 659-681
- [33] He, J. H., A Simple Approach to One-Dimensional Convection-Diffusion Equation and its Fractional Modification for E Reaction Arising in Rotating Disk Electrodes, *Journal of Electroanalytical Chemistry*, 854 (2019), 113565